The Photon-Assisted Cascaded Electron Multiplier Operation in CF_4 for Ion Backflow Suppression

F. D. Amaro, J. F. C. A. Veloso, J. M. F. dos Santos, A. Breskin, R. Chechik, and A. Lyashenko

Abstract—The operation of the recently introduced Photon Assisted Cascaded Electron Multiplier (PACEM) in CF_4 is investigated. The PACEM uses the VUV scintillation produced in the electron avalanches of the first multiplier of the cascade to transfer the signal to the subsequent ones. The VUV scintillation induces the emission of a large number of photoelectrons from a CsI photocathode placed on the top-surface of the second multiplier. The photoelectrons are further multiplied in the subsequent stages of the cascade, resulting in efficient signal amplification. A mesh, set at a fixed voltage, is placed between the first and the second multipliers to block the charge transfer between them, thus suppressing all the ion backflow (IBF) heading to the first cascade element. The PACEM electrically isolates the first multiplier of the cascade and only the ions produced in the electron avalanches of the first element may flow back into the drift region. Operating in CF_4, absolute IBFs as low as ∼1 ion per primary electron are achieved for drift fields of 0.1 kV/cm, while for fields of 0.5 kV/cm the absolute IBF is ∼10 ions/primary electron. This corresponds to an IBF of 10^{-4} at gains of 10^4, for Time Projection Chambers (TPC) operating conditions, and IBFs of ∼10^{-5} at gains of 10^6 for Gaseous Photomultipliers (GPM) operating conditions.

I. INTRODUCTION

THE Photon-Assisted Cascaded Electron Multiplier (PACEM) [1] was developed as an alternative for blocking avalanche-induced ions in cascaded gaseous electron multipliers. The avalanche originated in the first element propagates to the subsequent ones solely via its photons which, in turn, induce photoelectrons in the next multiplier of the cascade, while the charge transfer between the first and second cascade elements is blocked by a mesh electrode placed between them. This optical coupling is only effective in highly scintillating gases such as the heavy noble gases [2], [3], excluding applications in mixtures with quenching gases [2]. The PACEM principle and operational characteristics were demonstrated in xenon [1], [3]; by a proper choice of the gas, geometry and electric fields, the photon-assisted propagation can be made very efficient, while the charge transport between the first and the second element is completely blocked [3].

F. D. Amaro and J. M. F. dos Santos are with the Physics Department, University of Coimbra, Coimbra, Portugal (e-mail: famaro@gian.fis.uc.pt; jmf@gian.fis.uc.pt).

J. F. C. A. Veloso is with the Physics Department, University of Aveiro, Aveiro, Portugal (e-mail: jveloso@fis.ua.pt).

A. Breskin, R. Chechik, and A. Lyashenko are with the Department of Particle Physics, The Weizmann Institute of Science, Rehovot, Israel (e-mail: amos.breskin@weizmann.ac.il; rachel.chechik@weizmann.ac.il; alexey.lyashenko@weizmann.ac.il).

Amongst the molecular gases, CF_4 is known to have a high scintillation output, either under bombardment by ionizing radiation [4] or produced in electron avalanches [5], having a significant component in the VUV region (peak around 170 nm) [4]. In addition, it is an important gas with many applications in high energy physics instrumentation and neutron detection. However, the scintillation produced in electron avalanches in CF_4 is lower than that achieved in xenon, which can be a drawback to the implementation of the PACEM concept in CF_4. On the other hand, the collection efficiency of photoelectrons emitted by solid photocathodes in gaseous atmosphere is a few times higher in CF_4 than in xenon [7], [8]. This effect is mainly due to the existence of vibrational excitation states in CF_4 that, at low electron impact energies, can compete efficiently with elastic scattering. As a result of the presence of this additional mechanism the electron energy may be reduced after just a few collisions to values that decrease the probability of returning to the photocathode [9]. This could compensate the lower scintillation output and result in a good performance of the PACEM in CF_4.

In the present work, the operation of the PACEM in pure CF_4 is investigated. The optical gain, i.e., the number of photoelectrons transferred through the second cascade element per primary electron, and the relative IBF, i.e., the number of ions flowing back to the drift region per primary electron, are studied as a function of applied voltages.

II. ION BACKFLOW IN GASEOUS ELECTRON MULTIPLIERS

The positive ions produced in electron avalanches of gaseous detectors may present a serious drawback to the detector performance. These ions slowly flow back into the conversion/drift region of the detector and pose limitations to its operation. In particular, the trapping of the ions in gaseous detectors is of particular relevance for the development of Time Projection Chambers (TPC) and Gaseous Photomultipliers (GPM).

In TPCs, the presence and accumulation of ions in the drift region can disturb the electric field, resulting in dynamic track distortions [10]. This effect is most important in high-multiplicity experiments, e.g., relativistic heavy-ion physics applications [11]. GPMs equipped with bi-alkali photocathodes for visible light detection are even more sensitive to the ion back flow; ions impinging the photocathode have a high probability of inducing secondary emission of electrons, creating a mechanism of positive feedback that limits the gain [12]. In addition, ions reaching the photocathode are also a cause for faster aging, limiting the operation of the GPM for extended periods of time.

The fraction of ions that reach the drift region relative to the total number of electrons collected at the anode of the detector
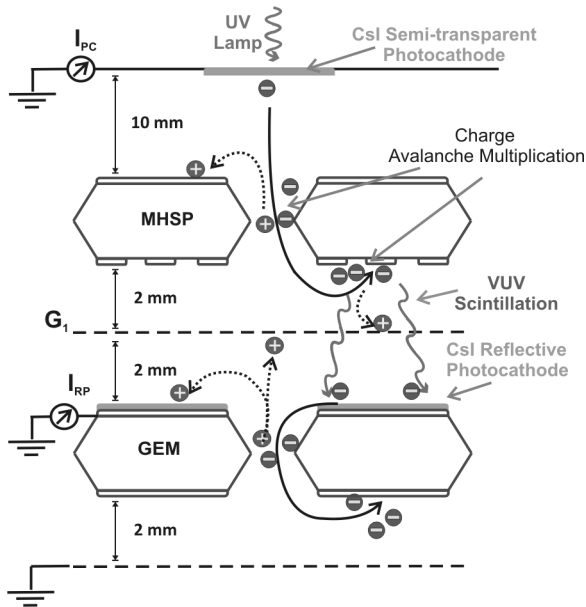
Fig. 1. Schematic view of the PACEM detector in a MHSP/GEM configuration.

Fig. 2. Top (upper view) and bottom (lower view) side of the MHSP.

is defined as the Ion Back Flow (IBF). A goal for IBF with values of 10^{-4} for gains of 10^4 and of 10^{-5} for gains of 10^6 has been established for TPCs [13] and GPMs [12], respectively. Short overviews of different methods and results obtained for IBF reduction are presented in [12] and [14]. So far, the lowest achieved values for IBF, 1.5×10^{-4} for a detector gain of 10^4 at a drift field of 0.2 kV/cm and 3×10^{-4} for a detector gain of 10^5 at a drift field of 0.5 kV/cm, were obtained in DC mode by electrostatic deviation and capture of the ions using a Micro Hole and Strip Plate (MHSP0) cascaded with Gas Electron Multipliers (GEM) [16], [17]. With this technique, a large amount of the total number of ions produced in the detector is trapped, and only a small fraction flows back to the drift region. The drawback of this method is that the absolute number of ions that reach the drift region increases when the gain of the detector increases, as more ions are produced.

A different approach to the IBF blocking was introduced with the Photon Assisted Cascaded Electron Multiplier (PACEM) detector [1], [3]. In this detector, only a fraction of the ions produced in the first cascade element will flow back to the drift volume. The ions produced in the last elements of the detector are completely blocked from flowing in to the drift region and the IBF is independent of the detector total gain. The operation of the PACEM in 1 bar of xenon has reached IBF values of $\sim 2 \times 10^{-4}$ for a detector gain of 10^4 and a drift field of 0.1 kV/cm and 10^{-5} for a detector gain of 10^6 and a drift field of 0.5 kV/cm [3].

III. EXPERIMENTAL METHOD AND SETUP

The PACEM used in this work is presented in Fig. 1, in a MHSP/GEM configuration, and is the one used in [3]. The MHSP and the GEM share the same production technique and are both made of a micro-perforated 50 μm Kapton® foil with a 28×28 mm^2 active area, covered on both sides with a 5 μm copper layer, gold coated. The main difference between these two structures is the strip pattern present on the bottom face of
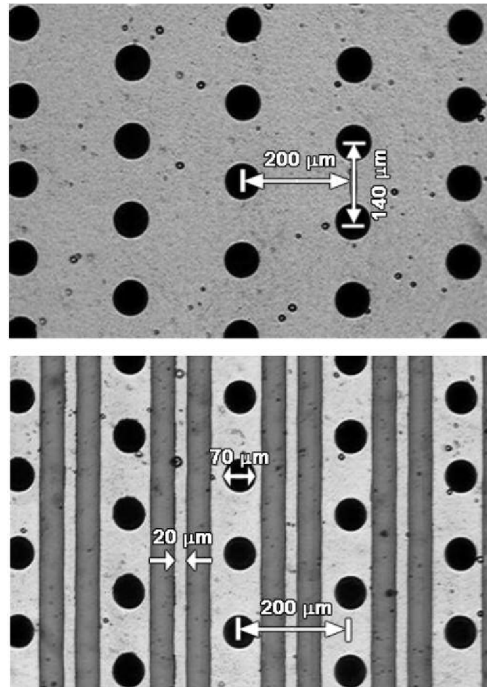
the MHSP. These strips are of two different and independent kinds: 100 μm wide cathode strips, perforated with 70 μm diameter biconical holes along the centre, and thinner, 20 μm wide anode strips etched between the cathode strips, Fig. 2. With this arrangement the MHSP presents two independent electron multiplication regions: inside the holes, which is established by the voltage difference between the top electrode and the cathode strips of the MHSP, V_{CT}, and in the region around the anode strips, which is established by the voltage difference between cathode and anode strips, V_{AC}. Compared to the GEM, the MHSP allows for an extra multiplication stage, resulting in higher scintillation and charge gains [1], [18]. In addition, depending on the electric field between the MHSP and the wire mesh, only $\sim 20\%$ of the anode-avalanche ions may drift back through the MHSP holes [19].

The scintillation produced in the avalanches of the MHSP induces the extraction of photoelectrons from the reflective CsI photocathode (2500 Å thickness) deposited on the top of the GEM. The stainless steel grid (80 μm diameter wires, 900 μm spacing), G_1, is connected to ground potential, blocking all the charge transfer between the MHSP and the GEM. The photoelectrons emitted by the CsI photocathode are transferred into the GEM holes, where they undergo multiplication. The avalanche electrons extracted from the holes are collected in the GEM bottom electrode. The reflective CsI Photocathode has very low sensitivity to charged-particles background, as discussed in [20].

For the measurements presented on this paper only the photoelectron current emitted by the reflective photocathode was recorded and there was no further photoelectron multiplication at the GEM holes. The grid G_1 was polarized while the top GEM electrode was at ground potential resulting in a extraction field of 1.0 kV/cm.

The detector was filled with CF_4 up to the pressure of 1 bar and operated in sealed mode. Prior to the filling, the detector was pumped down to a pressure of 10^{-6} mbar. During the operation of the detector, the CF_4 was continuously purified using non-evaporable getters, SAES St707. All the electrodes of the detector were independently biased. The present studies were performed operating the PACEM in current mode.

The primary electron current, I_{PC0}, is due to the photoelectron emission from the semitransparent photocathode placed above a 10 mm long drift region as shown in Fig. 1. This photocathode is composed by a 250 Å CsI layer deposited on a 5 mm thick quartz window, pre-coated with a 100 Å Al layer to ensure electrical contact trough the whole surface of the photocathode. An Hg(Ar) UV lamp is used to produced the primary electrons that are extracted from the photocathode into the gas by the electric field in the drift region. Since the semitransparent photocathode is grounded, the electric field is determined by the voltage of the MHSP top electrode. The currents on the semitransparent and reflective photocathode were measured using Keithley 610C electrometers.

We define the optical gain as the ratio between the number of photoelectrons extracted from the reflective photocathode due to the gas scintillation and the number of primary electrons emitted by the semitransparent photocathode. As the current measured at the reflective photocathode, I_{RP}, includes the contribution from both photoelectrons induced by the gas scintillation and photoelectrons induced by the direct exposure of the reflective photocathode to the UV photons emitted by the Hg lamp, I_{RP0}, the optical gain is given by

$$\text{Optical Gain} = \frac{I_{RP} - I_{RP_0}}{I_{PC_0}}. \tag{1}$$

Both I_{RP0} and I_{PC0} are measured for null electric fields in the MHSP, i.e., $V_{CT} = V_{AC} = 0$ V, and in the GEM, i.e., $\Delta V_{GEM} = 0$ V, and extraction field of 1.0 kV/cm in the region between the reflective photocathode and the wire mesh G_1. This value was found to ensure good extraction efficiency in the gas, above 90% [7].

The optical gain depends, amongst other factors, on the scintillation produced in the gas, on the photocathode quantum efficiency, on the solid angle subtended by the photocathode and on the photoelectron collection efficiency.

We define the absolute IBF as the number of ions flowing back to the drift region per primary electron, IBF/pe. In our setup, the absolute IBF is obtained by measuring the current at the semitransparent photocathode, I_{PC}. This current includes both the primary photoelectron current emitted by the photocathode and the current due to the positive ions produced in the MHSP avalanches that flow back to the drift region, I_{ions}. Therefore

$$\frac{\text{IBF}}{pe} = \frac{I_{ions}}{I_{PC_0}} = \frac{I_{PC} - I_{PC_0}}{I_{PC_0}}. \tag{2}$$

The IBF is obtained dividing the absolute IBF by the total gain of the cascade multiplier.

IV. EXPERIMENTAL RESULTS AND DISCUSSION

We have investigated the optical gain as a function of voltage difference between cathode and anode strips of the MHSP, V_{AC}, for different values of voltage difference applied to the MHSP
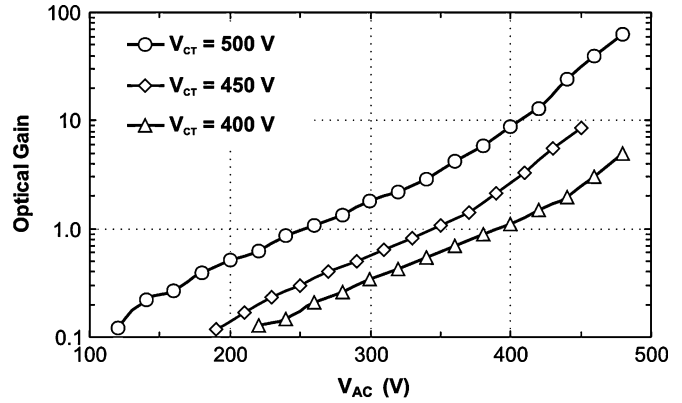

Fig. 3. PACEM optical gain in CF_4 as a function of V_{AC} for different V_{CT} voltages and for $E_{Drift} = 0.1$ kV/cm.
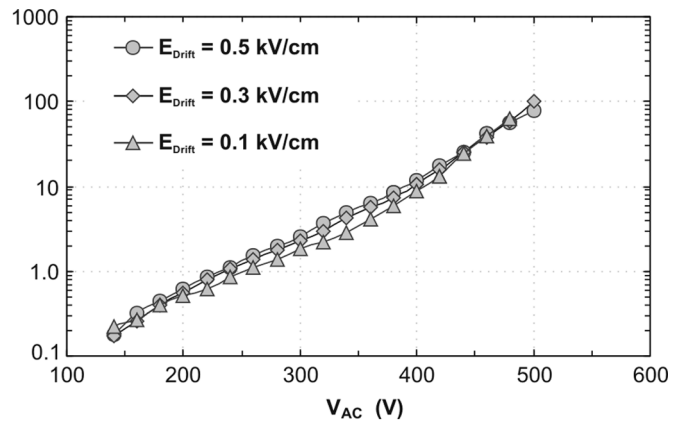

Fig. 4. PACEM optical gain in CF4 as a function of V_{AC} voltage for V_{CT} voltage of 500 V and different drift electric fields.

holes, V_{CT}, Fig. 3, and for different drift electric fields, Fig. 4. The results of Figs. 3 and 4, at low V_{AC} values, show that a GEM as the first element of the PACEM will not lead to optical gains high enough for an effective operation of the PACEM, presenting optical gains well below 1. Values similar to those achieved with the PACEM operating in GEM mode ($V_{AC} = 0$ V) were obtained by the authors of [2], using a GEM coupled to a CsI photocathode in a Kr atmosphere. The additional charge and scintillation gain achieved in the anode strips of the MHSP results in a fast increase in optical gain, which may reach values as high as 100.

Compared to the same conditions of operation in xenon, the optical gains obtained in CF_4 are lower, denoting the lower scintillation output achieved in CF_4. Nevertheless, values above 10 are achieved for V_{CT} and V_{AC} above 450 V, and maximum values achieved are comparable of those obtained when operating in pure xenon. The results of Fig. 4 also show that the optical gain is almost independent on the drift electric field.

To ensure that no primary charge is lost during the first multiplication stage, a relatively large gain on this stage is required (>10). On the PACEM detector this takes place at the MHSP holes, where, for the operational conditions presented on this paper, the gain is above 70 [21]. In addition, during previous work done with the PACEM detector operating at pulse mode in xenon, no energy resolution degradation from the first to the
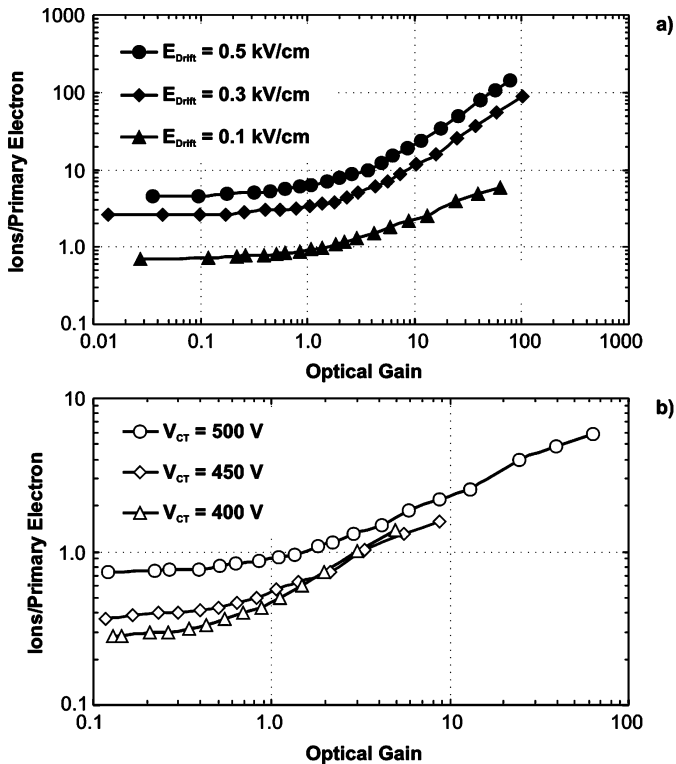
Fig. 5. Absolute IBF, ions reaching the semitransparent photocathode per primary electron, as a function of the PACEM optical gain for $V_{CT} = 500$ V and different drift electric fields (a) and for drift field of 0.1 kV/cm and different V_{CT} voltages (b).

second stage was observed [1], confirming that the gain on the first multiplication stage is large enough to assure full detection efficiency of the primary charge.

The absolute IBF was investigated as a function of optical gain for drift electric fields of 0.5 and 0.1 kV/cm (GPMs and TPCs operating conditions, respectively), Fig. 5. For GPM operating conditions, $E_{Drift} = 0.5$ kV/cm, 24 ions per primary electron were measured to reach the photocathode at an optical gain of 12. The operation of the PACEM with a triple-GEM coupled to a reflective photocathode [7], [22] as the second stage of the cascade multiplier may achieve a total gain of 10^6 with an IBF value of 2.4×10^{-5}. The same consideration can be made for the TPC operating conditions ($E_{Drift} = 0.1$ kV/cm) for which we have measured 2.5 ions per primary electron at an optical gain of 13. This value results in an IBF of 2.5×10^{-4} for total gains of 10^4. These figures are very close to the goal established for the operation conditions of these devices. Comparing to the PACEM operation in xenon, the operation in CF4 leads to the similar levels of ion blocking capability.

V. CONCLUSION

We have demonstrated the capability of the PACEM operating in CF4. The obtained results show that CF4 presents good scintillation and photoelectron extraction capabilities enabling to achieve optical gains as high as 100. The ion blocking capability of the PACEM in CF4 allows the reduction of the number of ions flowing back to the drift region per primary electron to 2.5 and 24 in TPC conditions ($E_{Drift} = 0.1$ kV/cm) and GPM conditions ($E_{Drift} = 0.5$ kV/cm), respectively. This corresponds

to IBF values of 2.5×10^{-4} and 2.4×10^{-5} at optical gains of about 12 for drift electric fields of 0.1 and 0.5 kV/cm and total cascade gains of 10^4 and 10^6, respectively. The obtained results are similar to those achieved for the PACEM operation in xenon, denoting that the lower scintillation output achieved in CF4 is compensated by the higher transmission efficiency of photoelectrons in CF4.

Future work in this area will involve the study of the pulse mode operation of the PACEM in CF4 and the study of the PACEM in other gases with high scintillation yields.

REFERENCES

[1] J. F. C. A. Veloso, F. D. Amaro, J. M. F. dos Santos, A. Breskin, A. Lyashenko, and R. Chechik, "The photon-assisted cascaded electron multiplier: A concept for potential avalanche-ion blocking," *J. Inst.*, vol. 1, p. P08003, 2006.

[2] A. Buzulutskov and A. Bondar, "Electric and photoelectric gates for ion backflow in multi-GEM structures," *J. Inst.*, vol. 1, p. P08006, 2006.

[3] J. F. C. A. Veloso, F. D. Amaro, C. D. R. Azevedo, J. M. F. Dos Santos, A. Breskin, A. Lyashenko, and R. Chechik, "PACEM: A new concept for high avalanche-ion blocking," *Nucl. Instrum. Meth. A*, vol. 581, pp. 261–264, 2007.

[4] A. Pansky, A. Breskin, A. Buzulutskov, R. Chechik, V. Elkind, and J. Va'vra, "The scintillation of CF4 and its relevance to detection science," *Nucl. Instrum. Meth. A*, vol. 354, pp. 262–269, 1995.

[5] M. M. F. R. Fraga, F. A. F. Fraga, S. T. G. Fetal, L. M. S. Margato, R. Ferreira Marques, and A. J. P. L. Policarpo, "The GEM scintillation in He-CF4; Ar—CF4; Ar-TEA and Xe—TEA mixtures," *Nucl. Instrum. Meth. A*, vol. 504, pp. 88–92, 2003.

[6] R. GernhWer, B. Bauer, J. Friese, J. Homolka, A. Kastenmiiller, P. Kienle, H.-J. K6rner, P. Maier-Komor, M. Miinch, R. Schneider, and K. Zeitelhack, "Photon detector performance and radiator scintillation in the HADES RICH," *Nucl. Instrum. Meth. A*, vol. 371, pp. 300–304, 1996.

[7] A. Breskin, A. Buzulustkov, and R. Chechik, "GEM photomultiplier operation in CF4," *Nucl. Instrum. Meth. A*, vol. 483, pp. 670–675, 2002.

[8] L. C. C. Coelho, H. M. N. B. L. Ferreira, J. A. M. Lopes, T. H. V. T. Dias, L. F. R. Ferreira, J. M. F. dos Santos, A. Breskin, and R. Chechik, "Measurement of the photoelectron-collection efficiency in noble gases and methane," *Nucl. Instrum. Meth. A*, vol. 581, p. 190, 2007.

[9] J. Escada, P. J. B. M. Rachinhas, T. H. V. T. Dias, J. A. M. Lopes, F. P. Santos, C. A. N. Conde, and A. D. Stauffer, "Photoelectron collection efficiency in Xe-CF4 mixtures," in *Proc. NSS & MIC Conf. Rec.*, 2007, vol. 1, pp. 585–589.

[10] M. Anderson *et al.*, *Nucl. Instrum. Meth. A*, vol. 499, p. 659, 2003.

[11] D. Friedrich, G. Melchart, B. Sadoulet, and F. Sauli, *Nucl. Instrum. Meth. A*, vol. 158, p. 81, 1979.

[12] A. Breskin, D. Mörmann, A. Lyashenko, R. Chechik, F. D. Amaro, J. M. Maia, J. F. C. A. Veloso, and J. M. F. dos Santos, "Ion-induced effects in GEM & GEM/MHSP gaseous photomultipliers for the UV and the visible spectral range," *Nucl. Instrum. Meth. A*, vol. 553, pp. 46–52, 2005, and references therein.

[13] F. Sauli, "GEM readout of the time projection chamber," *CERN-EP-TA1 Int. Rep.*, Jul. 29, 1999.

[14] J. F. C. A. Veloso, F. D. Amaro, J. M. Maia, A. V. Lyashenko, A. Breskin, R. Chechik, J. M. F. dos Santos, O. Bouianov, and M. Bouianov, "MHSP in reversed-bias operation mode for ion blocking in gas-avalanche multipliers," *Nucl. Instrum. Meth. A*, vol. 548, pp. 375–382, 2005, and references therein.

[15] J. M. Maia, J. F. C. A. Veloso, J. M. F. dos Santos, A. Breskin, R. Chechik, and D. Mörmann, "Advances in the micro-hole & strip plate gaseous detector," *Nucl. Instrum. Meth. A*, vol. 504, pp. 364–368, 2003.

[16] A. V. Lyashenko, A. Breskin, R. Chechik, J. F. C. A. Veloso, J. M. F. dos Santos, and F. D. Amaro, "Advances in ion back-flow reduction in cascaded gaseous electron multipliers incorporating R-MHSP elements," *J. Inst.*, vol. 1, p. P10004, 2006.

[17] A. V. Lyashenko, A. Breskin, R. Chechik, J. F. C. A. Veloso, J. M. F. Dos Santos, and F. D. Amaro, "Further progress in ion back-flow reduction with patterned gaseous hole—Multipliers," *J. Inst.*, vol. 2, p. P08004, 2007.

[18] F. D. Amaro, J. F. C. A. Veloso, A. Breskin, R. Chechik, and J. M. F. dos Santos, "Operation MHSP multipliers in high pressure noble-gas," *J. Inst.*, vol. 1, p. P04003, 2006.

[19] J. M. Maia, D. Mörmann, A. Breskin, R. Chechik, J. F. C. A. Veloso, and J. M. F. dos Santos, "Avalanche-ion backflow reduction in gaseous electron multipliers based on GEM/MHSP," *Nucl. Instrum. Meth. A*, vol. 523, pp. 334–344, 2004.

[20] D. Mormann, A. Breskin, R. Chechik, and B. K. Singh, "On the efficient operation of a CsI-coated photon detector," *Nucl. Instrum. Meth. A*, vol. 471, pp. 333–339, 2001.

[21] H. Natal da Luz, J. F. C. A. Veloso, F. D. Amaro, L. F. Requicha Ferreira, J. M. F. dos Santos, A. Breskin, and R. Chechik, "MHSP operation in pure xenon," *Nucl. Instrum. Meth. A*, vol. 552, pp. 259–262, 2005.

[22] D. M. ormann, M. Balcerzyk, A. Breskin, R. Chechik, B. K. Singh, and A. Buzulutskov, "GEM-based gaseous photomultipliers for UV and visible photon imaging," *Nucl. Instrum. Meth. A*, vol. 504, pp. 93–98, 2003.